CHAPTER 5

CHARACTERIZATION OF NANOPARTICLES

5 CHARACTERIZATION OF NANOPARTICLES

5.1 Introduction

The characterization of the nanoparticles is essential before proceeding for the cell culture studies and invivo studies. The characterization of nanoparticles is performed for predicting the reproducible characteristics of the prepared nanoparticle formulation. The optimized nanoparticles were characterized for particle size, zeta potential, drug entrapment efficiency, invitro release, surface morphology, DSC. Various techniques for characterization of nanoparticles include:

- Photon correlation spectroscopy (PCS) based on the diffraction light scattering (DLS) for particle size and distribution.
- The surface characteristics like charge is examined by measurement of zeta potential, surface morphology by transmission electron microscopy (TEM).
- The amount of the drug present in the nanoparticles can be estimated by evaluation of the entrapment efficiency and is estimated by well known techniques of spectrophotometry and chromatography.
- The invitro release of the drug from the nanoparticles influences the cytotoxicity pattern and the invivo pharmacokinetic and pharmacodynamic behavior and is estimated by spectrophotometric or chromatographic methods.
- Differential scanning calorimetry (DSC) is used for thermal characteristics to determine the crystalline or amorphous nature of the ingredients.
- The surface hydrophilicity of the nanoparticles influences the cellular uptake and also the invivo pharmacokinetic behavior of the nanoparticles. (Sahoo et. al, 2002) Polyvinyl alcohol resides on PLGA nanoparticles surface, even on repeated washing. The hydrophobic segments of PVA penetrate into the organic phase and remain entrapped into the polymeric matrix of the nanoparticles (F. Boury et, 1995). The surface PVA imparts the hydrophilicity to the nanoparticles and in our study is essential from perspective of the conjugation of Transferrin to the nanoparticle surface. The PVA is estimated using the colorimetric iodine reaction estimated spectrophotometrically. (D.P.Joshi et al, 1979)

Table 5.1 Materials and Equipments

Material	Source
Water (distilled)	Prepared in laboratory by distillation
Bichinconinic acid (BCA) protein Assay Kit	Banglore Genei, India
Glacial acetic acid, potassium dihydrogen phosphate, disodium hydrogen phosphate, potassium chloride, potassium hydroxide, sodium chloride, sodium hydroxide.	S.D.Fine chemicals, Mumbai, India
HPLC grade methanol, glacial acetic acid, acetonitrile	S.D.Fine chemicals, Mumbai, India
Nuclepore Polycarbonate membrane 2 μm 25mm	Whatman, USA
Polyvinyl alcohol	Sigma Chemicals, USA
Equipments	**Make**
Calibrated pipettes of 1.0 ml, 5.0 ml and 10.0 ml, volumetric flasks of 10 ml, 25 ml, 50 ml and 100 ml capacity, Funnels (i.d. 5.0 cm), beakers (250 ml) and other requisite glasswares	Schott & Corning (India) Ltd., Mumbai
Analytical balance	AX 120, EL 8300, Shimadzu Corp., Japan
pH meter	Pico^{+} Labindia, Mumbai, India
Cyclomixer, three blade stirrer	Remi Scientific Equipments, Mumbai
Cooling Centrifuge	3K 30, Sigma Laboratory centrifuge, Osterode, GmBH.
Lyophilizer	DW1, 0-60E, Heto Drywinner, Denmark
UV-Visible Spectrophotometer	Shimadzu UV-1601, Japan
Spectrofluorimeter	RF-540, Shimadzu corporation, Japan
Particle size and zeta potential analyzer	NanoZS, Malvern Instruments, U.K.
Transmission electron microscope	Morgagni, Philips, Netherlands
Differential Scanning Calorimeter	Mettler DSC 20, Mettler Toledo, Switzerland
HPLC system	LC 20-AT prominence, Shimadzu Corp., Japan

5.2 Methods

5.2.1. Particle size, zeta potential and drug entrapment efficiency

A 2.0 mg sample of lyophilized nanoparticles was suspended in distilled water, and the particle size and zeta potential were measured using the principle of laser light scattering with zeta sizer (Nano-ZS, Malvern Instruments, UK). The observations are tabulated in table 5.2 and figures 5.1 to 5.4.

To determine the amount of Etoposide and Temozolomide entrapped in the NPs, 2mg of NPs were added to 2 ml of acetonitrile and subjected to shaking at room temperature for 4hrs for complete dissolution of PLGA for extraction of drug from the nanoparticles. For Etoposide, the resulting system was centrifuged at 5000rpm for 15mins to remove the precipitated components. The supernant was further diluted with acetonitrile and estimated using UV spectrophotometry at 283nm. For Temozolomide, the resulting system was diluted with mobile phase {methanol: acetic acid (0.5%) (10:90)} and centrifuged at 5000rpm for 15mins to remove the precipitated components. The supernatant was analyzed after injection into the HPLC system.

The % drug entrapment efficiency (EE) was calculated using the following expression.

% EE = (Amount of drug in the NPs/drug added in the formulation) * 100

The results are recorded in table 5.2

5.2.2. In-vitro drug release

The invitro drug release of the nanoparticles of temozolomide was performed in phosphate-buffer saline (PBS) pH 7.4 at 37°C. (Shen Gao et al 2007) The release studies for etoposide nanoparticles in phosphate buffer saline pH 7.4 + 0.1%w/v polysorbate-80. (Jagdish Singh, 2000) Nanoparticles equivalent to 1mg drug were suspended in 10 ml of release media in a screw capped tubes, which were placed in a horizontal shaker bath maintained at 37°C and shaken at $60min^{-1}$. At specific time intervals following incubation samples were taken out and centrifuged at 15000rpm for 30min. The residue (settled nanoparticles) were collected and dissolved in acetonitrile. Temozolomide

nanoparticles were estimated by the HPLC method. Etoposide nanoparticles were analyzed by UV spectrophotometer. The amount of the drug released was calculated using the following equation:

$$\% \text{ Drug released} = 1 - \frac{\text{Amount of drug in nanoparticles settled}}{\text{Amount of drug initially taken}} \times 100$$

The release of drug from the unconjugated and conjugated nanoparticles is shown in fig. 5.5 and fig. 5.6 for etoposide and temozolomide respectively.

5.2.3. Transmission electron microscopy

Nanoparticles were dispersed in de-ionized water at a concentration of 1mg/ml. To measure the morphology and size distribution of nanoparticles, a drop of sample was placed onto a 300-mesh copper grid coated with carbon. Approximately 2 min after deposition, the grid was tapped with filter paper to remove surface water and air-dried. Negative staining was performed using a droplet of 0.5% w/v phosphotungstic acid. Transmisssion electron microscopy was performed using Morgagni 268, Philips (Netherlands) transmission electron microscope. The TEM images for unconjugated and Tf conjugated nanoparticles for Etoposide and Temozolomide are shown in figure 5.7 and 5.8 respectively.

5.2.4 Differential Scanning Calorimetry

DSC of ETP, PLGA, PLGA-ETP-NP, TMZ and PLGA-TMZ-NP were performed using differential scanning calorimetry instrument. Thermograms were analyzed using Mettler Toledo star SW 7.01/8.10. An empty aluminium pan was used as the reference for all measurements. During each scan, 3-5 mg of sample was heated, in a hermetically sealed aluminium pan, at a heating rate of 10° C/min, from 35-50° C to 300° C, under a nitrogen atmosphere. Figures 5.9 a, b, c show the thermograms for PLGA, ETP and PLGA-ETP-NP. Figures 5.10 a, b show the thermograms of TMZ, PLGA-TMZ-NP

5.2.5 Residual PVA

The amount of PVA associated with nanoparticles was determined by a colorimetric method based on the formation of a colored complex between two adjacent hydroxyl groups of PVA and an iodine molecule (D.P. Joshi et al, 1979). Briefly, 2 mg of lyophilized nanoparticle sample was treated with 2 ml of 0.5 M NaOH for 15 min at 60 °C. Each sample was neutralized with 900 µl of 1 N HCl and the volume was adjusted to 5 ml with distilled water. To each sample, 3 ml of a 0.65 M solution of boric acid, 0.5 ml of a solution of I_2/KI (0.05 M/0.15 M), and 1.5 ml of distilled water were added. Finally, the absorbance of the samples was measured at 690 nm after 15 min incubation. A standard plot of PVA was prepared under identical conditions.

5.2.6 Characterization of 6-coumarin nanoparticles

Fluorescent nanoparticles of 6-coumarin were characterized for particle size, zeta potential, entrapment efficiency, Surface Tf density and residual PVA and the results are recorded in table 5.3. The estimation of 6-coumarin was done by spectroflurorimetry at excitation and emission wavelength of 430nm and 485nm respectively

5.3 Results and Discussions

5.3.1 Particle size, zeta potential and drug entrapment efficiency

The particle size, zeta potential and drug entrapment efficiency (%EE) for PLGA-ETP-NP and Tf-ETP-NP are recorded in table 5.2. The particle size and zeta potential are shown in fig. 5.1 and 5.2 respectively.

Table 5.2: Characterization of optimized Tf conjugated and unconjugated PLGA nanoparticles of Etoposide and Temozolomide

Parameter	* PLGA-ETP-NP	# Tf- PLGA-ETPNP	*PLGA-TMZ-NP	#Tf- PLGA-TMZ-NP
Mean particle size (nm)	149 ± 8	162.1 ± 12	138 ± 7	153.8±14
Zeta potential (mV)	-9.8 ± 1.3	-11.69±0.8	-7.8 ± 1.7	-13.6 ± 3.1
Entrapment efficiency (%)	65.4 ± 2.2 %	57.7 ± 3.1	70.3 ± 2.4	61.4 ± 2.9

(Mean ± S.D., $n = 3$)

* PLGA-ETP-NP- Etoposide loaded PLGA nanoparticles

Tf-PLGA-ETP-NP – Tf conjugated Etoposide loaded PLGA nanoparticles

* PLGA-TMZ-NP- Temozolomide loaded PLGA nanoparticles

Tf-PLGA-TMZ-NP – Tf conjugated Temozolomide loaded PLGA nanoparticles

Figure 5.1: Particle size distribution plots of Etoposide loaded PLGA nanoparticles, before and after Tf conjugation.

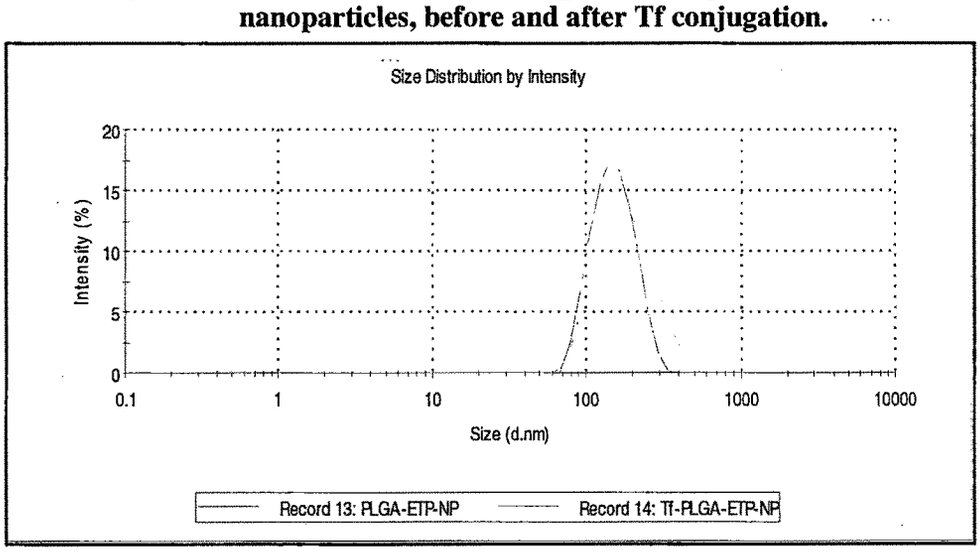

Figure 5.2: Zeta potential plots of Etoposide loaded PLGA nanoparticles, before and after Tf conjugation

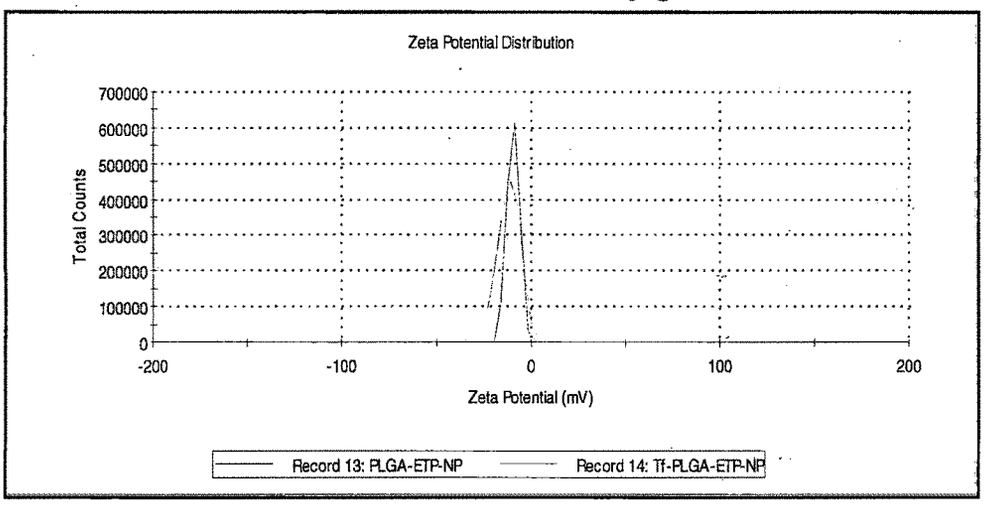

Mean particle size and zeta potential of PLGA-ETP-NP and Tf-PLGA-ETP-NP were found to be 149 ± 8nm and -9.8 ± 1.3mV and 162.1 ± 12nm and -11.69±0.8mV respectively. Increase in the particle size after transferrin conjugation was due to transferrin conjugated. The %EE for PLGA-ETP-NP and Tf-PLGA-ETP-NP was found to be 65.4 ± 2.2 % and 57.7 ± 3.1% respectively. The reduced drug entrapment efficiency for Tf-PLGA-ETP-NP may be due to dissociation of the drug on the surface of PLGA-ETP-NP during the Tf conjugation process.

Similarly, the particle size and zeta potential for PLGA-TMZ-NP and Tf-PLGA-TMZ-NP are recorded in table 5.1. The particle size and zeta potential are shown in fig. 5.3 and 5.4 respectively. Mean particle size and zeta potential of PLGA-TMZ-NP were found to be 138 ± 7nm and -7.8 ± 1.7, while the Tf-PLGA-TMZ-NP demonstrated 153.8±14nm particle size and -13.6 ± 3.1mV zeta potential. The %EE for PLGA-TMZ-NP and Tf-PLGA-TMZ-NP was determined to be 70.3 ± 2.4% and 61.4 ± 2.9% respectively.

Figure 5.3: Particle size distribution plots of Temozolomide loaded PLGA nanoparticles, before and after Tf conjugation

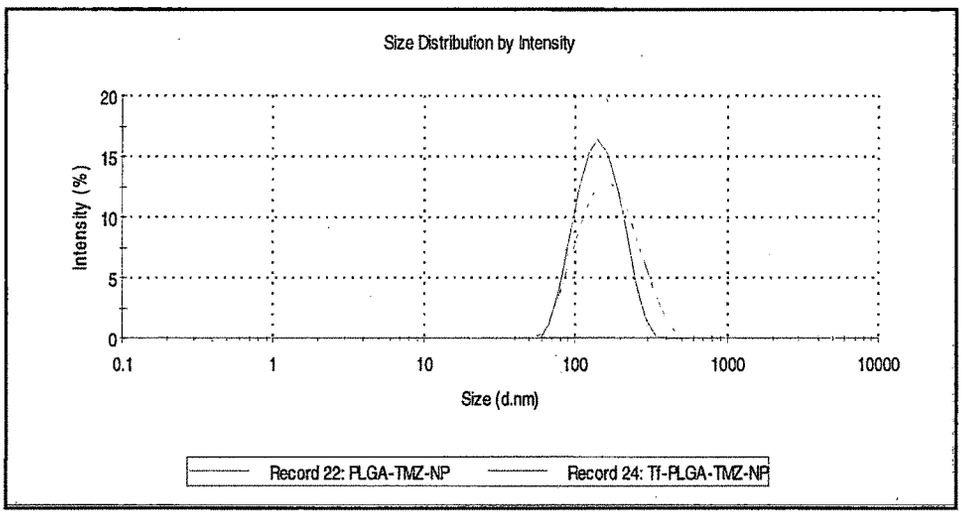

Figure 5.4: Zeta potential plots of Temozolomide loaded PLGA nanoparticles, before and after Tf conjugation

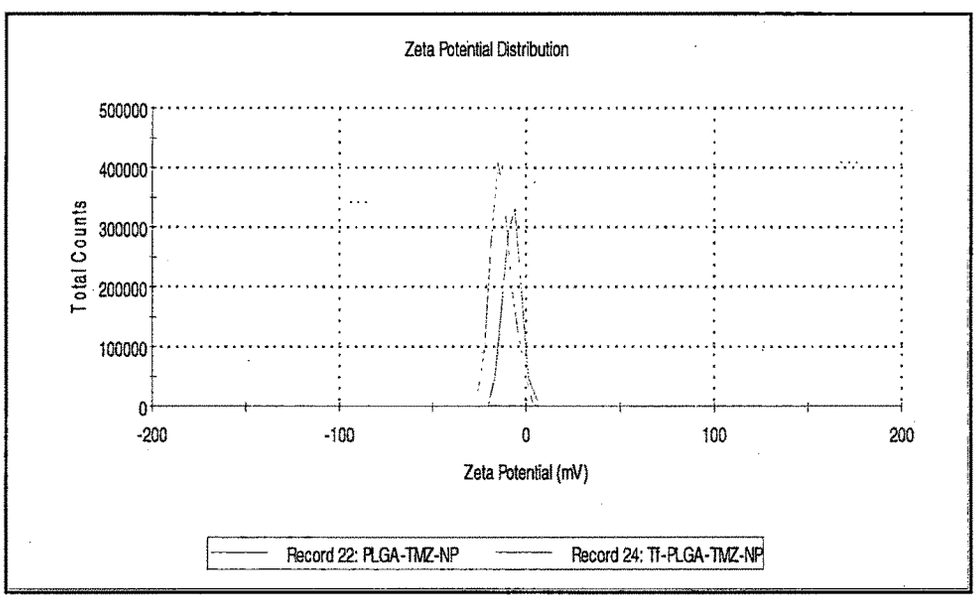

5.3.2 In-vitro Drug Release

The release of the drug from PLGA is by the degradation of polymer by hydrolysis of its ester linkages in the presence of water. In general the mechanism by which active agent is released from a delivery vehicle is a combination of diffusion of the active agent from the polymer matrices, bulk erosion of the polymer, swelling and degradation of the polymer. The degradation of PLGA is slow, therefore the release of etoposide and temozolomide from NPs may depend on drug diffusion and PLGA surface and bulk erosion or swelling (Mu and Feng 2003).

Figure 5.5: In-vitro release of etoposide from etoposide loaded PLGA NPs before and after conjugation with Tf.

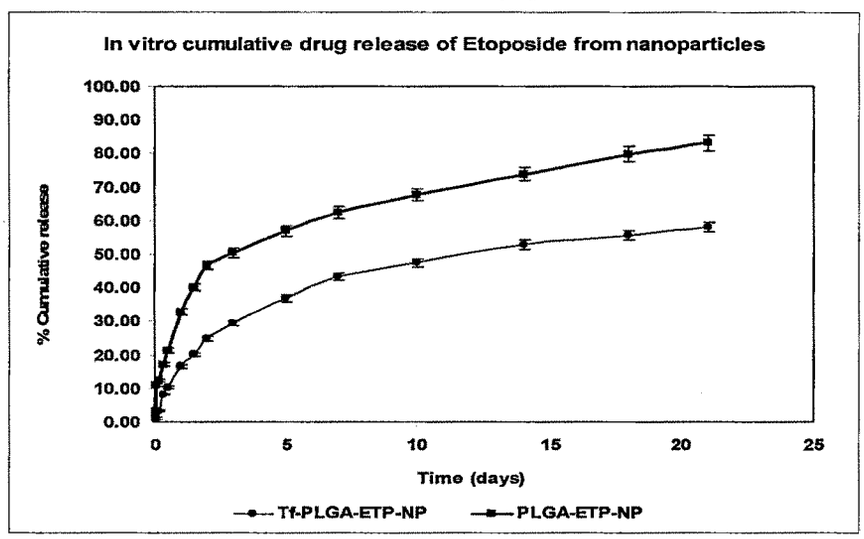

(Mean ± S.D., $n = 3$)
PLGA-ETP-NP- Etoposide loaded PLGA nanoparticles
Tf-PLGA-ETP-NP – Tf conjugated Etoposide loaded PLGA nanoparticles

The release studies of etoposide from the optimize nanoparticle batch was conducted in phosphate buffer pH 7.4 + 0.1%w/v polysorbate-80. The release curves of PLGA-ETP-NP and Tf-PLGA-ETP-NP are shown in fig. 5.5. For PLGA-ETP-NP there was an initial burst release of about 21% in 12hrs (0.5 days) and then there was a lag phase and about 80% release resulted in 21 days. A high initial burst was observed for unconjugated nanoparticles which can be attributed to the immediate dissociation and dissolution of drug adhered on the surface and located near the surface of the NPs (Magenheim et al.,

1993). After that, in lag phase, the release is mainly due to the erosion of the polymer matrix and further diffusion of drug molecules through the polymeric matrix of the NPs. The matrix material would require time to erode in the aqueous environment than the release mechanisms of surface release, resulting in the prolonged release. (F. Esmaeili et al., 2008)

The burst effect was absent in Tf-PLGA-ETP-NP and the release in 21 days was found to be about 60%. The absence of burst release with Tf-conjugated NPs may be due to absence of drug on the surface of conjugated NPs.

Similarly, the release studies of temozolomide from the optimize nanoparticle batch were conducted in phosphate buffer pH 7.4. The release curves of PLGA-TMZ-NP and Tf-PLGA-TMZ-NP are shown in fig. 5.6.

Figure 5.6: In-vitro release of temozolomide loaded PLGA nanoparticles before and after conjugation with Tf

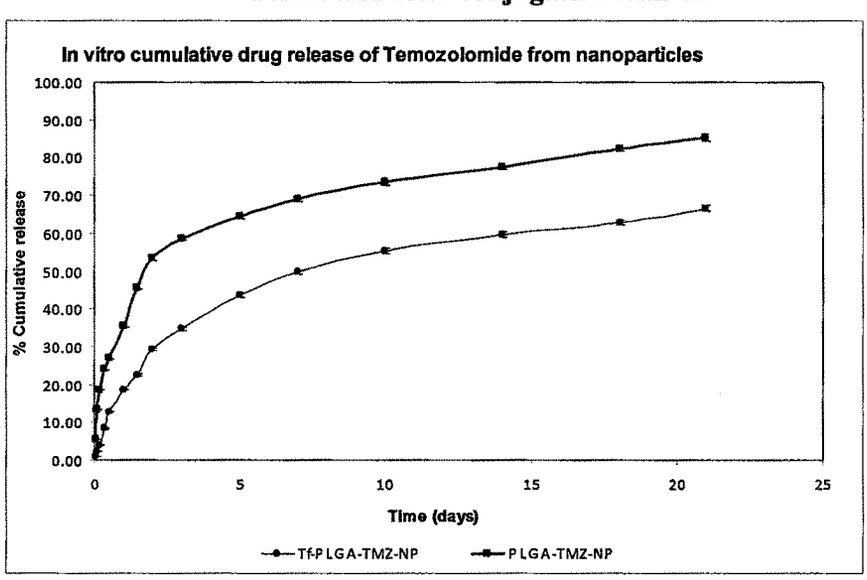

(Mean ± S.D., $n = 3$)
PLGA-TMZ-NP- Temozolomide loaded PLGA nanoparticles
Tf-PLGA-TMZ -NP – Tf conjugated Temozolomide loaded PLGA nanoparticles

For PLGA-TMZ-NP the initial burst was about 27% in 12 hrs (0.5days) and lag phase showing about 75% release in 14days and further about 85% in 21 days. The cumulative

drug release for Tf-PLGA-TMZ-NP was found to be devoid of initial burst and with about 68% drug release in 21 days.

5.3.3 Transmission Electron Microscopy

The TEM images for etoposide and temozolomide nanoparticles are shown in figure 5.7 and 5.8 respectively. TEM images of the unconjugated and conjugated NPs showed spherical NPs with smooth surfaces. In the Tf-conjugated nanoparticles a faint corona/lining appears around the nanoparticle surface differentiating from the unconjugated nanoparticles.

Figure 5.7: Morphology of Etoposide nanoparticles using TEM

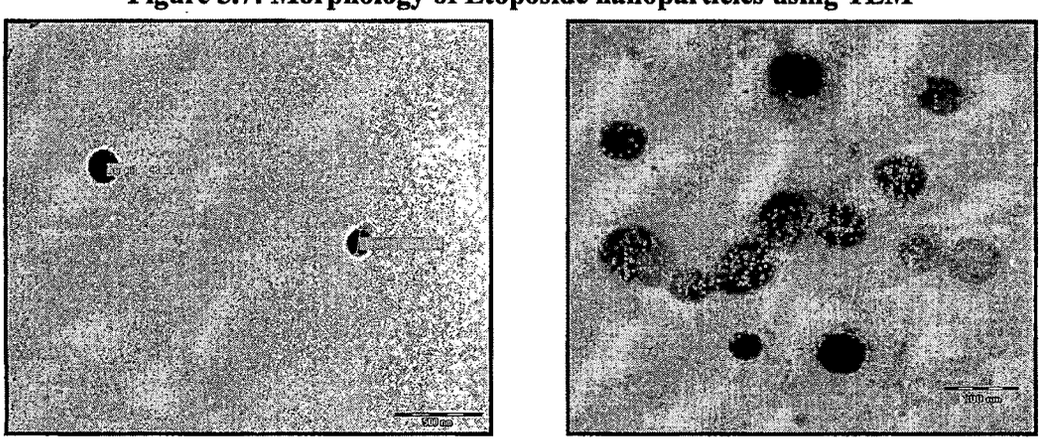

(a) PLGA-ETP-NP (b) Tf-PLGA-ETP-NP

Figure 5.8: Morphology of Temozolomide nanoparticles using TEM

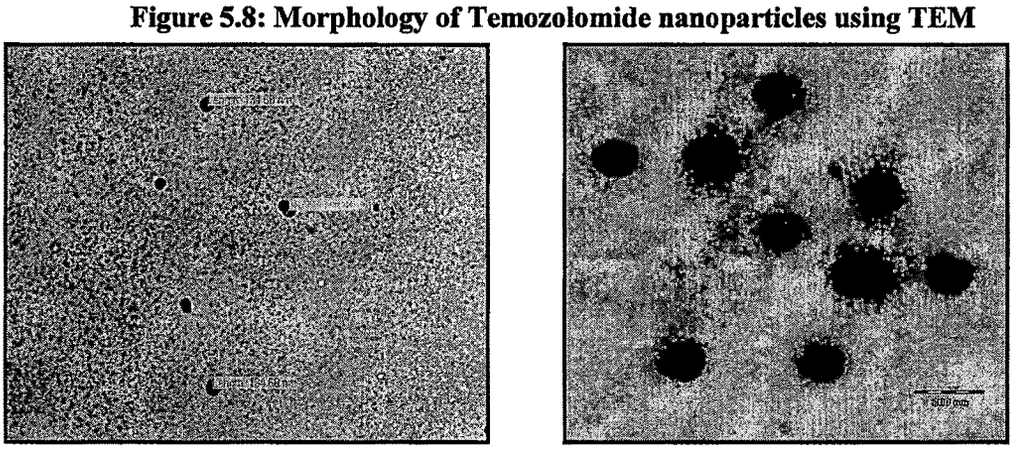

(a) PLGA-TMZ-NP (b) Tf-PLGA-TMZ-NP

5.3.4 Differential Scanning Calorimetry

DSC studies were performed to investigate the physical state of the drug in the NPs, because this aspect could influence the in vitro and in vivo release of the drug from the systems. Different combinations of drug/polymer may coexist in the polymeric carriers, such as: (i) amorphous drug in either an amorphous or a crystalline polymer and (ii) crystalline drug in either an amorphous or a crystalline polymer. Moreover, a drug may be present either as a solid solution or solid dispersion in an amorphous or crystalline polymer. PLGA shows a Tg and not a Tm (melting point), indicating the presence of the polymer in amorphous form.

The DSC thermogram of PLGA, Etoposide and PLGA-ETP-NP are shown in figure 5.9.

Figure 5.9: DSC thermograms for Etoposide

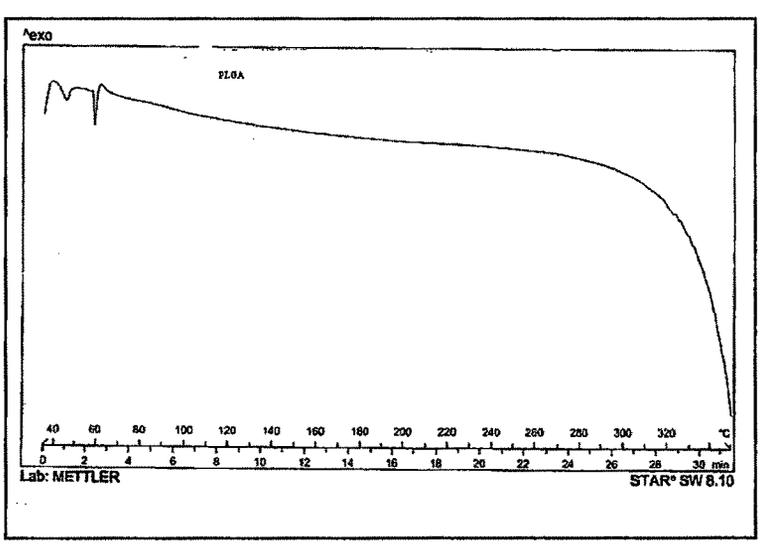

(a) PLGA

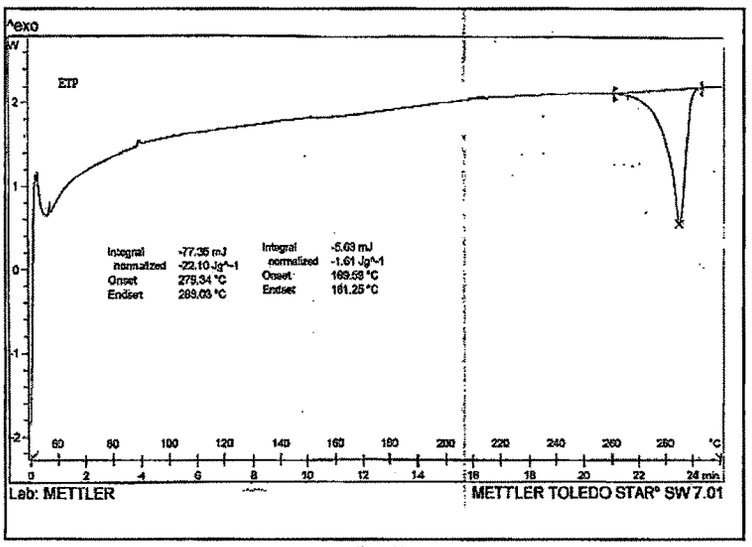

(b) ETP

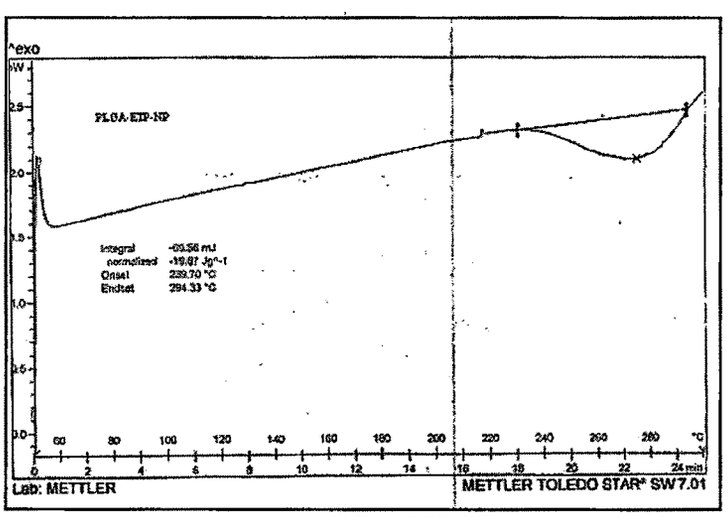

(c) PLGA-ETP-NP

DSC thermogram of plain Etoposide shown in figure 5.9b depicts a sharp melting peak from 279-289°C, indicating the crystalline nature of the drug. The drug in the amorphous form is entrapped in the nanoparticles. For PLGA-ETP-NP, as shown in figure 5.9c, the peak of Etoposide stretched from 239.7-294°C indicating the conversion of Etoposide

into amorphous state during the nanoparticle formulation and thereby entrapped in the PLGA polymer.

The DSC thermograms for Temozolomide (TMZ) and PLGA-TMZ-NP are shown in figure 5.10.

Figure 5.10: DSC thermograms for Temozolomide

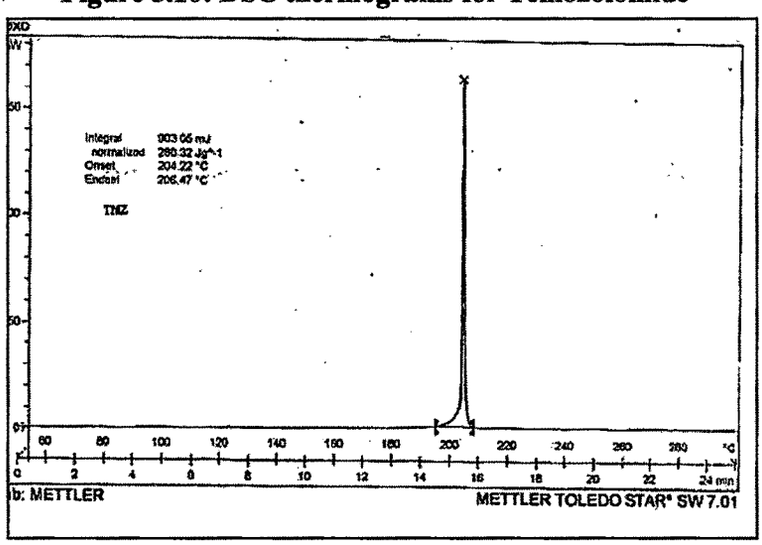

(a) TMZ

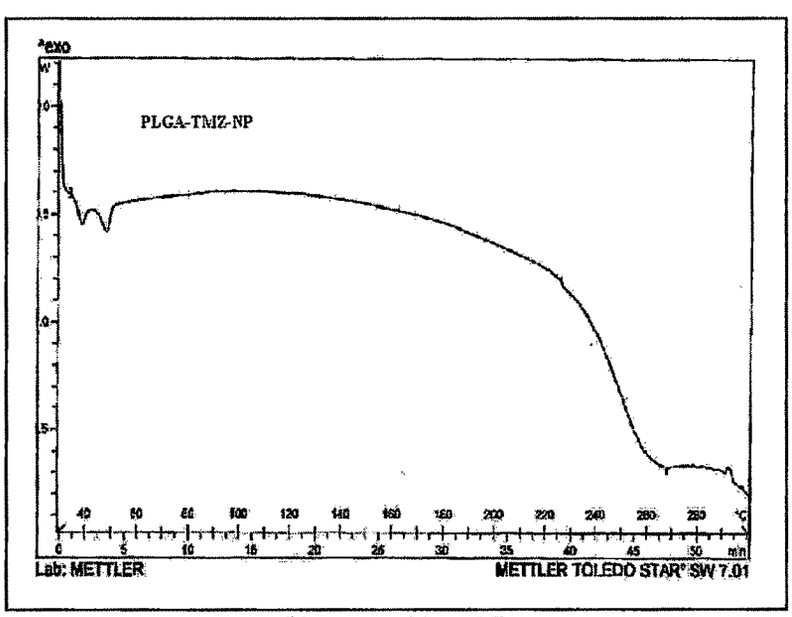

(b) PLGA-TMZ-NP

Similarly, Temozolomide (TMZ) showed a characteristic endothermic peak from 204.22-206.47°C as shown in fig. 5.10a. No drug peak was seen for PLGA-TMZ-NP as shown in figure 5.10b indicating the presence of Temozolomide in the nanoparticles in the amorphous state entrapped in the polymer (F. Esmaeili et al., 2008)

5.3.5 Residual PVA

The residual PVA associated with the nanoparticle surface was 7.8 ± 1.6 % & 7.2 ± 1.1 % w/w of nanoparticles for unconjugated etoposide and temozolomide nanoparticles and 5.7 ± 1.0 % & 5.2 ± 0.8 % w/w of nanoparticles for transferrin conjugated etoposide and temozolomide nanoparticles respectively.

5.3.6 Characterization of 6-coumarin nanoparticles

Unconjugated and Tf conjugated fluorescent NPs encapsulating 6-coumarin required for studying cellular uptake of NPs by C6 glioma cells were prepared and characterized by the same methods used for drug loaded NPs and the results are recorded in Table 5.3.

Table 5.3: Characterization of 6- coumarin nanoparticles

Character	6-coumarin nanoparticles	
	Unconjugated	Tf conjugated
Particle size (nm)	151.6 ± 4	168.2 ± 9
Zeta potential (mV)	-7.9 ± 1.7	-12.4 ± 1.2
Entrapment Efficiency	93.14 ± 2.71	85.48 ± 1.43
Surface Tf (µg /mg)	----	34.1 ± 2.7
Residual PVA (% w/w)	7.8 ± 2.0	5.5 ± 1.5

6-coumarin loaded unconjugated NPs and Tf-conjugated NPs had a particle size of 151.6 ± 4 nm and 168.2 ± 9nm and zeta potential of -7.9 ± 1.7 mV and -12.4 ± 1.2 mV respectively. Tf conjugated NPs had 34.1 µg Tf /mg of nanoparticles. The entrapment efficiency as evaluated using spectrofluorimetry was found to be 93.14 ± 2.71 and 85.48

± 1.43 for unconjugated and conjugated 6-coumarin nanoparticles. The residual PVA was found to be 7.8 ± 2.0 % and 5.5 ± 1.5 % for unconjugated and transferrin conjugated nanoparticles respectively. The particle size, zeta potential, the surface density of Tf and residual PVA of 6-coumarin NPs were found to be similar to the drug loaded NPs. So it is expected that their cellular uptake would be similar to that of the drug loaded NPs.

5.4 Conclusions

After characterization we can conclude that the unconjugated and transferrin conjugated nanoparticles of etoposide and temozolomide have small particle size (<200nm) suitable for intravenous administration. A prolonged release was observed for both unconjugated and conjugated nanoparticles of etoposide and temozolomide. The smooth and spherical surface of nanoparticles was confirmed from TEM. The DSC studies indicate the presence of the drug in nanoparticles in the amorphous form.

The unconjugated and Tf conjugated nanoparticles of etoposide and temozolomide were further subjected to stability studies according to ICH guidelines (Chapter 6).

References

- D.P. Joshi, Y.L. Lan-Chun-Fung and J.W. Pritchard , Determination of poly (vinyl alcohol) via its complex with boric acid and iodine. *Anal. Chim. Acta* **104** (1979), pp. 153–160

- F. Boury, T. Ivanova, I. Panaiotov et al., Dynamic properties of poly (D,L-lactide) and polyvinyl alcohol monolayers at the air/water and dichloromethane air/water interfaces. J. Colloid. Interf. Sci. **169** (1995), pp. 380–392

- F. Esmaeili et al., PLGA nanoparticles of different surface properties: Preparation and evaluation of their body distribution, International Journal of Pharmaceutics 349 (2008) 249–255

- Jagdish Singh, Mathew J. Schaefer, 2000. Effect of Isopropyl Myristic Acid Ester on the Physical Characteristicsand In Vitro Release of Etoposide from PLGA Microspheres, AAPS PharmSciTech 2000; 1(4) article 32

- Sanjeeb K. Sahoo, Jayanth Panyam, Swayam Prabha and Vinod Labhasetwar. Residual polyvinyl alcohol associated with poly (lactide-co-glycolide) nanoparticles affects their physical properties and cellular uptake. Journal of Controlled Release Volume 82, Issue 1, 18 July 2002, Pages 105-114

- Shen Gao, He Zhang 2007. Temozolomide/PLGA microparticles and antitumor activity against Glioma C6 cancer cells in vitro. Int. J. of Pharm., 329;1-2, 122-128